

# AGE AND COMPOSITION OF THE GRÃO PARÁ GROUP VOLCANICS, SERRA DOS CARAJÁS

ALLAN K. GIBBS\*, KARL R. WIRTH\*,  
WALTER K. HIRATA\*\* e WILLIAM J. OLSZEWSKI JR.\*\*\*

**ABSTRACT** Metavolcanic rocks underlying the Serra dos Carajás iron ore deposits yield Late Archean ages, and show isotopic and chemical evidence of assimilation of some of the continental crust through which they erupted. The lower metavolcanic sequence of the Grão Pará Group North and East of the Serra Norte iron deposits is bimodal, with dominant basalts, basaltic andesites, and trachyandesites, and subordinate rhyolite tuffs and flows at several stratigraphic levels. Most volcanic rocks are of medium to low metamorphic grade, with more intense metamorphism and deformation along the northern contact with gneisses and granitoid rocks (Xingu Complex). Thickness of the volcanic section is not known, but may be about 4-6 km. The basalts and basaltic andesites yield a whole rock Rb-Sr isochron age of  $2,687 \pm 54$  Ma. The initial Sr isotopic ratio of  $0.7057 \pm 0.0010$  demonstrates that the basalts incorporated material that had history of elevated Rb/Sr ratios. Sm-Nd ratios in the mafic rocks are too tightly clustered to yield an isochron, and using the zircon age of 2,758 Ma they yield  $\epsilon_{Nd}$  values varying from +4.6 to -7.0, averaging +0.6. The Nd and Sr isotopic data and the trace and rare-earth element compositions of these mafic rocks are all consistent with contamination of mantle-derived melts by significant but variable amounts of diverse older continental crust. The stratigraphy, geochemical and isotopic compositions show that the group originated on extending, older continental crust. An age-terrane boundary must exist between this Archean continental terrane and the apparently ensimatic Early Proterozoic greenstone belts of the northern Amazonian craton.

**RESUMO** As rochas metavulcânicas sob os depósitos de minério de ferro do Grupo Grão Pará são do Arqueano Superior e contém evidências químicas e isotópicas de assimilação de parte da crosta continental pela qual se injetaram. A seqüência metavulcânica inferior do Grupo Grão Pará ao Norte e Este da Serra Norte é bimodal, contém basaltos, andesitos basálticos, traquiandesitos e quantidades menores de riólitos, que ocorrem em vários níveis estratigráficos. A maioria das rochas vulcânicas é de grau metamórfico médio a baixo. O metamorfismo e a deformação são mais intensas ao longo do contato, na parte norte, com gnaisses e granitos (Complexo Xingu). A espessura da seção vulcânica não é conhecida, mas calcula-se que deve atingir de 4 a 6 km. Os basaltos produzem uma isócrona Rb-Sr de rocha total de  $2.687 \pm 54$  Ma, estatisticamente de idade similar à idade dos zircões dos riólitos. A razão inicial de Sr de  $0,7057 \pm 0,0010$  demonstra que o material incorporado pelo basalto tinha razão Rb/Sr elevada. A relação Sm-Nd nos basaltos é agrupada de tal maneira que é impossível produzir isócronas. Utilizando o valor de idade de 2.758 Ma, encontraremos valores de  $\epsilon_{Nd}$  de +3,2 a -1,9, com uma média de +0,2. Os dados isotópicos de Nd e Sr, bem como os elementos menores e terras raras destas rochas máficas, demonstram que uma porção significativa, porém variável, de material continental mais velho foi assimilado. A estratigrafia e a composição geoquímica e isotópica das rochas demonstram que o Grupo Grão Pará foi formado sobre crosta continental mais antiga. Deve haver uma separação entre esta crosta continental e os *greenstone belts* do Proterozóico Inferior do Escudo das Guianas.

**INTRODUCTION** The Grão Pará Group is the lowest stratigraphic unit of the Serra dos Carajás belt. It consists of a lower metavolcanic sequence, the Carajás Formation iron ore deposits, and an upper metavolcanic and metasedimentary sequence. This paper summarizes the results of field studies, and petrographic, geochemical, and isotopic analyses of the volcanic rocks in the Grão Pará Group surrounding the Serra Norte iron deposits. Important observations and conclusions are that: rhyolites are present along with the basalts and basaltic andesites; the volcanic suite resembles modern bimodal continental volcanics rather than Archean greenstone belt volcanics; and the volcanism occurred at about 2.75 Ga, much earlier than previously suspected.

This is a report on work in progress. Details of the field observations are in Gibbs *et al.* (1985). Previous summaries of the regional geology of Serra dos Carajás and its ore

deposits were provided by Silva *et al.* (1974), Santos (1981), Hirata *et al.* (1982), Beisiegel (1982), Farias & Saueressig (1982), Bernardelli (1982), Tassinari *et al.* (1982), Cordani *et al.* (1984), Amaral (1984), and Santos & Loguercio (1984).

**LITHOSTRATIGRAPHY** Several stratigraphic units have been recognized in the Carajás belt, though none have formally-defined stratotypes. The major units were reviewed by Hirata *et al.* (1982). The Grão Pará Group is on the periphery of the belt and consists of metavolcanic and metasedimentary rocks, including banded iron formations. A quartz-rich sandstone unit occupies the central part of the belt (Fig. 1). Between these two units is a poorly-exposed, low-elevation zone with interbedded volcanic, tuffaceous, and clastic and chemical sedimentary rocks. This zone includes the upper metavolcanic and

\* Institute for the Study of the Continents and Department of Geological Sciences, Cornell University, Ithaca, NY 14853, USA (Gibbs, present address: NASA, Johnson Space Center, SN 4, Houston, TX 77058, USA)

\*\* Rio Doce Geologia e Mineração S.A., Tv. Lomas Valentinas, 2717, Marco, CEP 66000, Belém, PA, Brasil

\*\*\* Department of Earth Sciences, University of New Hampshire, Durham, NH 03824, USA

metasedimentary sequence of the Grão Pará Group and may also include the contact between the Grão Pará Group and the overlying sandstone unit. Our traverses provided samples of the various rock types in the Grão Pará Group, and a general impression of the typical order of succession of lithologies within it.

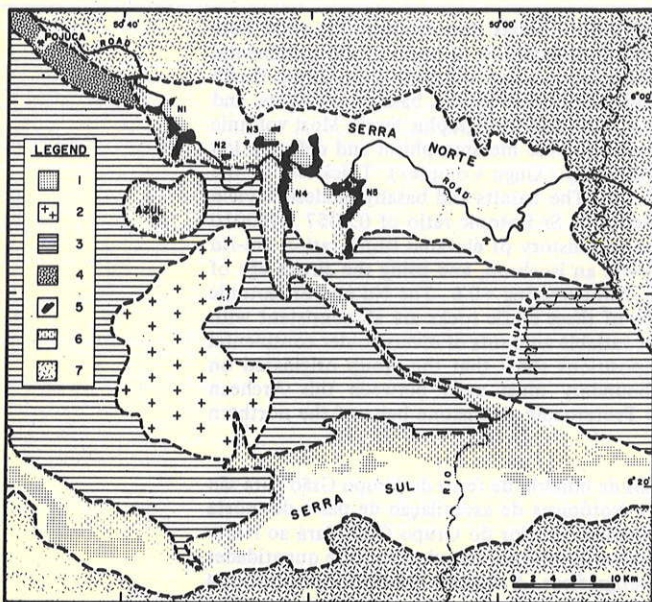


Figure 1 – Lithological map of the Serra dos Carajás region. Key: 1 – savanna areas, generally developed over iron formation, 2 – Serra dos Carajás Granite, 3 – unnamed sandstone unit, 4 – Pojuca Sequence, 5 – Carajás Formation itabirite, in Serra Norte, 6 – Grão Pará Group: Lower Metavolcanic Sequence (unpatterned), Upper Sequence (vertical dashes), 7 – Xingu Complex

**Lower Metavolcanic Sequence** The lower metavolcanic sequence is well exposed in saprolite roadcuts along the Parauapebas – Serra Norte road and along the creek northeast of N1. Massive, vesicular, and porphyritic basalt flows and mafic agglomeratic breccias predominate, but there are also breccias of massive and flow-banded felsic volcanics, stratified felsic tuffs, and quartz-porphyritic rhyolite flows. Felsic volcanics occur in several zones interlayered with more abundant basalts along both traverses. Basalts are well exposed between N4 and N5, east of N5, and in many of the CVRD drill cores. The basalts are typically massive in outcrop, without obvious flow structures. They vary in vesicularity, grain size, and phenocryst content, with variations on scales from a few meters to a few tens of meters.

Felsic volcanics account for about 10-15% of the volcanic exposures in Serra Norte. These include lapilli and finer-grained crystal and vitric tuffs and homogeneous flows. Thicknesses of these felsic units are not precisely known, but must be on the order of several tens of meters. Most are porphyritic with quartz, plagioclase, and, in some cases, altered ferromagnesian phenocrysts. They weather red to white and form relatively hard saprolite. Relatively fresh felsic volcanic rocks are pale green, grey, black, or red.

Red might also be due to weathering. Bipyrarnidal quartz phenocrysts, typically corroded, help in the identification of felsic volcanic saprolites.

The thickness of the lower metavolcanic sequence is not known. It varies from about 1.5 to over 15 km in map width, in both Serra Norte and Serra Sul. Folds and faults have been mapped within the iron ore zones, and similar deformation probably occurs within the volcanic section. Exposures of the lower metavolcanic sequence average about 5-8 km in map width, and layering typically dips 55-70 degrees, these features suggest that the stratigraphic thickness of the lower metavolcanic sequence might be about 4-6 km.

**Carajás Formation** The Carajás Formation includes the major banded iron formations, which are about 100-400 m thick (Tolbert *et al.* 1971, Beisiegel 1982). Primary textures are well exposed on the savannas, in spite of leaching of the jasper bands. In many places the beds are folded, and in some cases broken, probably due to early soft-sediment deformation.

Volcanic rocks in the vicinity of the iron deposits have been referred to as “upper” and “lower” units according to their structural position with reference to the iron formation. This is a structural, rather than stratigraphic distinction. Contacts between the volcanics and iron formations are visible in the iron-exploration drill cores. Scoriaceous and brecciated flow tops in the underlying basalts have chlorite, quartz, pyrite, and other secondary minerals filling the voids. Iron formation and mafic volcanic rocks are interbedded in some of the drill cores, demonstrating the stratigraphic conformability of the Carajás Formation with the rest of the Grão Pará Group (Beisiegel 1982).

**Upper Sequence** A topographically-low zone separates the Carajás Formation from the overlying sandstone unit. Many of the exposures of this zone in Serra Norte are schistose, showing intense deformation. The zone includes the upper sequence of the Grão Pará Group, and may also include rocks that should be grouped with the overlying sandstone unit. Further field work is needed to define the zone's stratigraphy and contacts. Maps and remote imagery of the Carajás belt suggest that about 1-3 km of relatively easily-eroded rocks typically separate the Carajás Formation from the overlying sandstone unit in the central part of the belt.

The creek between N2 and N3 exposes the section through and above the Carajás Formation. Most of these exposures are of foliated saprolites derived from fine-grained tuffs, tuffaceous siltstones, phyllites, cherts, greywackes, and less abundant mafic flows. Distinctive conglomerates with angular clasts of banded iron formation and fine-grained tuffs occur as float just above the banded iron formation south of N1 and between N2 and N3. Several prominent beds of quartz-rich sandstone appear to be conformable with chloritic metatuffs.

The Azul manganese mine is in a topographically low region about 6 km in diameter. The manganese deposits form a gentle anticline in the south-central part of this area (Bernardelli 1982). Exposures of saprolite in exploration pits contain evidence of soft-sediment deformation (folds and penecontemporaneous small-scale faults) in siltstones, shales, manganeseiferous beds, and fine-grained

sandstones. Along the eastern margin of this region, siltstone and shale, with cross-bedded sandstone interbeds, and a distinctive mud-matrix slump breccia are overlain with uncertain conformity by massive quartz sandstones. Cherts with stylonites and weathered carbonate occur as float along with the sandstones. Our limited observations in the Azul area suggest that the Azul sequence is a structural dome that may be correlated with the upper sequence of the Grão Pará Group.

Near N1 the road to Pojuca passes through saprolites derived from basaltic flows and flow breccias. Fine to medium grained tuffaceous metasediments and some polymict conglomerates are exposed further to the northwest. Faults obscure the stratigraphic position of these tuffaceous schists. This section is lithologically similar to the section above N2-N3, suggesting that the section northwest of N1 might be another exposure of the upper sequence.

**Unnamed Sandstone Unit** The central portions of the Carajás belt are occupied by a dominantly sedimentary sequence, including prominent cross-bedded quartz-rich sandstones as well as fine-grained clastic and chemical sedimentary rocks. These were previously referred to as the Gorotire or Rio Fresco Formations, but recent work by Ramos *et al.* (1984) and Figueiras & Villas (1982) suggest that these correlations may not be correct, and so they are referred to as an unnamed unit of post-Grão Pará Group clastic sedimentary rocks. These recent works list its lithologies as orthoquartzites, sublithic and lithic arenites, and subordinate siltstones and phyllites. Lithic fragments in the arenites are ferruginous fragments and microcrystalline cherts.

**Other Stratigraphic Units** Gneisses adjacent to the Grão Pará Group are assigned to the Xingu complex, broadly defined to include all of the high and medium grade gneisses and granitoid rocks in the surrounding lowlands. The complex has generally been considered Archean, although most of the isotopic ages for it are Trans-Amazonian or younger (Amaral 1974, Gomes *et al.* 1975, Cordani *et al.* 1984). The Grão Pará Group is considered to be unconformable on this complex, and on older greenstone belts and granulite belts that are structurally included in the complex.

The Pojuca and Salobo sequences are amphibolite-grade metamorphosed sedimentary and volcanic rocks, and include a prominent magnetite iron-formation, exposed northwest of the Grão Pará Group. Both have copper mineralization in magnetite and silicate facies iron formations. Only a few hundred meters of section surrounding the ore zones at these prospects have been described in detail. These sequences are structurally separated from the Grão Pará Group, and although their stratigraphic relations to the Grão Pará Group have been obscured by deformation and metamorphism, some (e.g. Medeiros Neto & Villas 1985) have speculated that these sequences might correlate with the Carajás Formation. Another copper sulphide prospect, Bahia, is located within the Carajás belt south of Pojuca. The Bahia section is not as deformed or metamorphosed as Pojuca, but many of the Bahia rocks have been hydrothermally altered. Volcanic rocks of the Bahia prospect analyzed by Ferreira Filho & Danni (1985) are comparable in petrography and major element composi-

tion to the Grão Pará Group metavolcanic rocks.

The Serra do Carajás Granite cuts the sandstone unit, and xenoliths of the sandstone are included in the granite. The granite has been dated at about 1.8 Ga (Gomes *et al.* 1975, Tassinari *et al.* 1982, Wirth *et al.* 1986). Mesozoic dolerite dikes are the youngest rocks of the region.

#### PETROGRAPHY OF THE GRÃO PARÁ GROUP (METAVOLCANIC ROCKS)

The basalts exposed in streams are mostly fine to medium grained. Variations in amounts and sizes of vesicles in the fine-grained volcanics help identify flow margins and interiors. Leucocratic patches, generally ovoid, about 0.5 to 2 cm in diameter, occur in saprolites derived from mafic volcanic rocks in several localities. They might be variolites, a second, megacrystic population of feldspar phenocrysts, or xenoliths.

Mafic metavolcanic rocks range from fine (<1 mm) to medium grained (1-3 mm) and were originally hypo to holocrystalline. Euhedral plagioclase occurs with lesser amounts of intergranular clinopyroxene. Interstitial, cloudy, and green-brown alteration minerals might represent former volcanic glass. Plagioclase feldspars in some samples exhibit sub-parallel flow structures. Subhedral and skeletal iron-titanium oxides are closely associated with secondary sphene and apatite. Amygdules and vesicles are typically filled with zoned assemblages of chlorite, quartz, calcite, epidote, and amphibole. Scapolite is associated with actinolite, chlorite and biotite in some of the mafic metavolcanic rocks.

Felsic metavolcanic rocks consist of 10-20% phenocrysts of quartz and feldspar and minor amounts of altered ferromagnesian minerals. The quartz phenocrysts are typically hexagonal bipyramids (<3 mm in diameter) with embayed and corroded boundaries. Feldspar phenocrysts are present in some of the rhyolites, strongly altered to clay and mica. One sample contains approximately 5-10% fresh subhedral plagioclase (An<sub>10-20</sub>). Rare zircon, allanite and opaque minerals are also present. A few samples contain subhedral and rectangular patches that are now composed of platy bundles of biotite and chlorite. These may represent the alteration products of former amphiboles. The groundmass is typically composed of patchy mosaics of granophyre, and includes varying amounts of small (<0.05 mm long) amphibole (?), biotite and chlorite. Granophyric rims are sometimes present around phenocrysts of quartz and feldspar. A few small amygdules are also present in some of the rhyolites, and these contain mineral assemblages similar to those found in the mafic rocks. Diffuse zones of chlorite, epidote and biotite also occur in some of the rhyolites. These may be zones of extreme alteration and recrystallization, or they may be former xenoliths.

Mineral assemblages in the mafic rocks indicate low grade metamorphic conditions. Metavolcanic rocks near the iron deposits still exhibit primary mineralogies and textures. Further to the north, along the contact with the Xingu Complex, the rocks were recrystallized in the upper greenschist to lower amphibolite facies, with abundant blue-green amphibole, fresh plagioclase, epidote and minor quartz. Most of the metavolcanic rocks are massive and do not exhibit a pronounced foliation or mineral segregation layering, although some are strongly foliated.

The Grão Pará Group has a general WNW-ESE trend. A major NW-SE fault and some subordinate faults in

other directions complicate the map pattern (Fig. 1a). The best evidence of the orientation of layering is exposed in the iron deposits, where dips are moderate to steep and of varying orientation. This regional trend is complicated by folds with approximately N-S axes and faults of various orientations. Our traverses within the volcanic sections were too widely separated to resolve strikes of the massive volcanic flow units. Faults visible on airphotos and radar imagery strike N-S and NW-SE, repeating the Grão Pará Group section, and obscuring its relation with the sandstones in the center of the belt. The road from N1 to Pojuca provides strong evidence of increasing metamorphic grade and intense shearing towards this northern contact, which is probably a fault.

**GEOCHEMISTRY** Analyses of 14 mafic and 4 felsic volcanic rocks (Table 1) indicate the range and typical compositions of the Grão Pará Group in the vicinity of Serra Norte (Fig. 2). Analyses of Grão Pará Group metabasalts from drill core in the upper part of the section have been published (Lemos & Villas 1983).

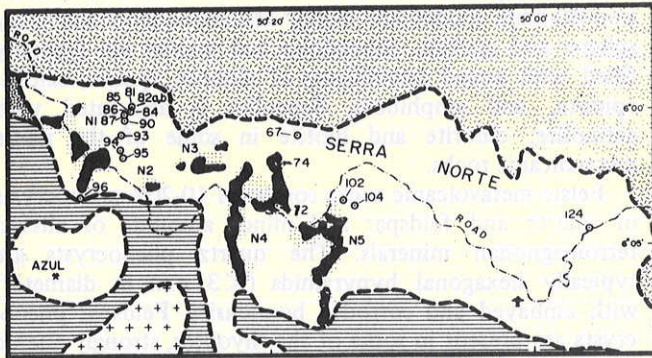


Figure 2 – Location map of samples collected for geochemical analysis in the Serra Norte region, Serra dos Carajás

The mafic rocks are classified according to their silica and alkali contents as basalts, basaltic andesites, and trachyandesites (Fig. 3a). Most of the trachyandesites are moderately potassic ( $K_2O > (Na_2O - 1.5\%)$ ), and are thus called shoshonites. One analysis plots in the andesite field, and has higher Th, U, and Ta, and lower Mg than the other mafic rocks. None of the analyses plot in the dacite field. The analyses confirm the bimodality of the volcanics in terms of silica content. Lemos & Villas (1983) analysed several rocks with 51-53%  $SiO_2$ , indicating that the absence of rocks with compositions between basalts and basaltic andesites is an artifact of our sample set.

Chemical variations in these rocks may be attributed to the mantle source compositions, assimilation of lithosphere or crust material during ascent, magma differentiation (fractional crystallization, magma mixing, etc.), early hydrothermal alteration, and metasomatism during regional metamorphism. Such influences have not yet been fully resolved, but much of the variation can probably best be accounted for by variations in extent of fractional crystallization and in the amounts and compositions of crustal contaminants.

The magnesium numbers of the mafic rocks have a restricted range (0.41 – 0.54), and do not correlate with Si or K. The Si, K, Rb, and Ba contents of the mafic rocks are positively correlated. Contents of K, Rb, and Ba are distinctly higher than in mafic volcanics of modern oceanic ridges, island arcs, or most Precambrian greenstone belts.

In spite of the petrographic and field evidence of synvolcanic hydrothermal alteration and regional metamorphism, the alkali ratios and most readily altered trace elements are not notably affected in most samples. Variations in K, Rb and Ba are correlated in the mafic rocks. Na contents are extremely low in several rhyolites and one basalt, probably due to alteration. Depletion of K and enrichment of Na in GB 84, and to a lesser extent in GB 86 might be due to sea-water metasomatic alteration (spilitization). Rb and Ba are also lower in these two samples than

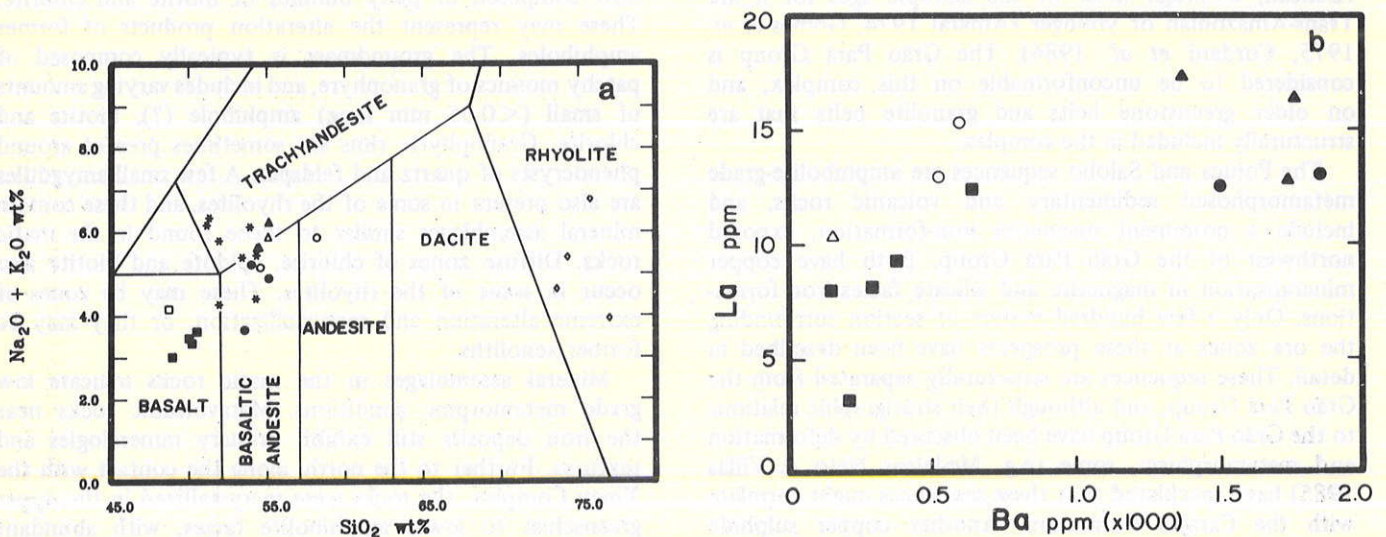


Figure 3 – Chemical variation diagrams for the Grão Pará Group volcanic rocks. Key to symbols: squares – basalts, circles – basaltic andesites, triangles – trachyandesites (in this case, shoshonites), diamonds – rhyolites. Open symbols are samples that might be altered. Samples plotted with asterisks are from Lemos & Villas (1983). a) Alkali-silica diagram, showing the bimodal range of silica contents, and the I.U.G.S. rock classification system. b) La – Ba variations in the mafic volcanic rocks. Note the positive correlation of La and Ba in the basalts and andesites, and the much higher Ba in the trachyandesites

Table 1 - Analyses of Grão Pará Group metavolcanic rocks. See appendix for description of analytical procedures

| Sample Location                | BASALTS    |            |             |            |             |            |            |            |            |            | BASALTIC & TRACHYANDESITES |             |            |            |            |            |            |             |  |  | RHYOLITES |  |  |  |  |
|--------------------------------|------------|------------|-------------|------------|-------------|------------|------------|------------|------------|------------|----------------------------|-------------|------------|------------|------------|------------|------------|-------------|--|--|-----------|--|--|--|--|
|                                | GB-90<br>a | GB-87<br>a | GB-82B<br>a | GB-81<br>a | GB-82A<br>a | GB-93<br>a | GB-67<br>b | GB-74<br>a | GB-86<br>a | GB-96<br>a | GB-104<br>c                | GB-102<br>c | GB-84<br>a | GB-72<br>f | GB-94<br>a | GB-95<br>a | GB-85<br>a | GB-124<br>d |  |  |           |  |  |  |  |
| SiO <sub>2</sub>               | 48.70      | 49.06      | 49.51       | 50.29      | 50.54       | 53.36      | 53.82      | 54.07      | 54.34      | 54.39      | 54.40                      | 54.77       | 55.03      | 57.69      | 72.79      | 73.79      | 74.60      | 77.52       |  |  |           |  |  |  |  |
| TiO <sub>2</sub>               | 0.81       | 0.83       | 1.52        | 1.55       | 1.33        | 0.84       | 0.76       | 0.86       | 0.76       | 0.97       | 0.88                       | 0.84        | 1.08       | 0.86       | 0.29       | 0.35       | 0.31       | 0.27        |  |  |           |  |  |  |  |
| Al <sub>2</sub> O <sub>3</sub> | 15.89      | 15.97      | 14.96       | 14.96      | 14.31       | 15.09      | 14.47      | 14.93      | 15.17      | 14.00      | 14.51                      | 15.02       | 14.25      | 13.91      | 11.16      | 11.39      | 11.61      | 12.64       |  |  |           |  |  |  |  |
| FeO*                           | 12.24      | 11.82      | 13.85       | 14.29      | 15.81       | 12.17      | 11.10      | 12.45      | 10.41      | 11.82      | 10.19                      | 9.58        | 11.18      | 10.52      | 8.26       | 6.83       | 3.37       | 5.04        |  |  |           |  |  |  |  |
| MnO                            | 0.19       | 0.19       | 0.17        | 0.19       | 0.39        | 0.22       | 0.52       | 0.32       | 0.19       | 0.21       | 0.62                       | 0.58        | 0.34       | 0.36       | 0.06       | 0.07       | 0.06       | 0.05        |  |  |           |  |  |  |  |
| MgO                            | 7.74       | 7.75       | 5.60        | 5.75       | 6.22        | 5.45       | 6.58       | 7.17       | 6.30       | 5.57       | 5.81                       | 5.96        | 4.84       | 4.85       | 1.74       | 1.39       | 0.31       | 1.20        |  |  |           |  |  |  |  |
| CaO                            | 10.84      | 10.80      | 9.86        | 9.66       | 7.74        | 8.78       | 7.14       | 4.10       | 7.13       | 7.14       | 6.50                       | 6.35        | 7.53       | 5.05       | 0.00       | 0.10       | 1.57       | 0.06        |  |  |           |  |  |  |  |
| Na <sub>2</sub> O              | 1.92       | 3.17       | 2.84        | 2.60       | 2.85        | 2.48       | 2.91       | 2.72       | 4.17       | 3.08       | 2.60                       | 3.48        | 4.52       | 2.66       | 0.07       | 0.08       | 2.05       | 0.09        |  |  |           |  |  |  |  |
| K <sub>2</sub> O               | 1.08       | 1.02       | 0.59        | 0.75       | 0.78        | 1.17       | 2.30       | 2.39       | 1.46       | 2.56       | 3.22                       | 2.73        | 0.37       | 3.16       | 4.51       | 5.28       | 4.63       | 3.87        |  |  |           |  |  |  |  |
| P <sub>2</sub> O <sub>5</sub>  | 0.08       | 0.09       | 0.12        | 0.15       | 0.09        | 0.08       | 0.07       | 0.06       | 0.05       | 0.07       | 0.04                       | 0.06        | 0.08       | 0.07       | 0.02       | 0.05       | 0.00       | 0.00        |  |  |           |  |  |  |  |
| Total:                         | 99.49      | 100.70     | 99.02       | 100.19     | 100.06      | 99.64      | 99.67      | 99.07      | 99.98      | 99.81      | 98.77                      | 99.37       | 99.85      | 99.12      | 99.90      | 99.33      | 98.51      | 100.74      |  |  |           |  |  |  |  |
| Loss on Ignition               | 1.91       | 1.95       | 0.43        | 0.68       | 0.81        | 1.62       | 2.09       | 3.11       | 1.07       | 1.67       | 2.15                       | 2.05        | 0.51       | 2.58       | 1.93       | 1.85       | 0.51       | 2.53        |  |  |           |  |  |  |  |
| Cr                             | 308        | 167        | 180         | 178        | 202         | 70         | 141        | 121        | 259        | 79         | 137                        | 102         | 102        | 77         | 6          | 17         | 9          | 3           |  |  |           |  |  |  |  |
| Ni                             | 133        | 78         | 57          | 66         | 59          | 82         | 63         | 29         | 66         | 81         | 61                         | 43          | 43         | 59         | 25         | 14         | 3          | 5           |  |  |           |  |  |  |  |
| Co                             | 62         | 47         | 56          | 56         | 57          | 57         | 50         | 45         | 45         | 51         | 44                         | 43          | 43         | 50         | 17         | 15         | 5          | 14          |  |  |           |  |  |  |  |
| Sc                             | 38         | 34         | 43          | 45         | 45          | 37         | 37         | 41         | 36         | 40         | 38                         | 43          | 43         | 37         | 1          | 2          | 3          | 6           |  |  |           |  |  |  |  |
| Ba                             | 213        | 636        | 151         | 290        | 376         | 594        | 1847       | 1499       | 522        | 1367       | 1736                       | 155         | 155        | 1759       | 1125       | 1604       | 1427       | 449         |  |  |           |  |  |  |  |
| Cs                             | 0.14       | 0.04       | 0.00        | 0.19       | 0.02        | 0.23       | 0.37       | 0.32       | 0.49       | 0.57       | 0.22                       | 0.06        | 0.06       | 0.35       | 0.06       | 0.12       | 0.11       | 0.31        |  |  |           |  |  |  |  |
| Rb**                           | 41         | 131        | 18          | 112        | 20          | 43         | 79         | 130        | 36         | 127        | 120                        | 101         | 101        | 48         | 61         | 78         | 97         | 6           |  |  |           |  |  |  |  |
| Sr**                           | 1.34       | 1.99       | 2.27        | 2.59       | 2.49        | 2.43       | 1.92       | 2.65       | 2.04       | 2.77       | 2.16                       | 2.16        | 2.94       | 3.21       | 14.75      | 14.98      | 12.41      | 10.53       |  |  |           |  |  |  |  |
| Hf                             | 0.15       | 0.35       | 0.48        | 0.44       | 0.41        | 0.34       | 0.28       | 0.55       | 0.30       | 0.41       | 0.33                       | 0.33        | 0.79       | 0.47       | 2.31       | 2.46       | 2.28       | 1.42        |  |  |           |  |  |  |  |
| Ta                             | 0.68       | 4.11       | 1.09        | 1.28       | 3.07        | 4.37       | 3.93       | 4.54       | 3.49       | 5.41       | 4.21                       | 4.57        | 6.08       | 27.97      | 27.90      | 23.07      | 15.05      | 15.05       |  |  |           |  |  |  |  |
| Th                             | 0.23       | 1.19       | 0.26        | 0.63       | 1.39        | 1.44       | 1.19       | 1.58       | 0.91       | 1.99       | 1.50                       | 1.32        | 2.17       | 5.93       | 6.08       | 5.02       | 4.13       | 4.13        |  |  |           |  |  |  |  |
| U                              | 3.2        | 12.4       | 8.0         | 8.2        | 9.3         | 15.3       | 13.1       | 12.5       | 13.0       | 17.4       | 12.9                       | 10.4        | 16.4       | 16.6       | 31.9       | 79.2       | 28.9       | 28.9        |  |  |           |  |  |  |  |
| La                             | 8          | 25         | 17          | 19         | 21          | 30         | 26         | 24         | 24         | 34         | 25                         | 22          | 22         | 30         | 34         | 60         | 157        | 55          |  |  |           |  |  |  |  |
| Ce                             | 12.84      | 11.82      | 11.82       | 12.23      | 12.23       | 13.58      | 11.97      | 12.34      | 12.34      | 12.34      | 12.99                      | 11.86       | 11.86      | 15.82      | 15.82      | 75.73      | 75.73      | 4.11        |  |  |           |  |  |  |  |
| Nd**                           | 1.88       | 2.93       | 3.55        | 3.67       | 3.72        | 3.41       | 2.83       | 3.06       | 2.81       | 3.88       | 2.90**                     | 2.95        | 3.07       | 3.39       | 3.68       | 6.73       | 12.85      | 4.11        |  |  |           |  |  |  |  |
| Sm                             | 0.63       | 0.96       | 1.15        | 1.16       | 1.08        | 1.01       | 0.81       | 0.92       | 0.66       | 1.00       | 0.80                       | 0.80        | 0.94       | 0.91       | 0.65       | 1.37       | 1.74       | 0.64        |  |  |           |  |  |  |  |
| Eu                             | 0.45       | 0.56       | 0.90        | 0.87       | 0.83        | 0.64       | 0.55       | 0.55       | 0.49       | 0.74       | 0.53                       | 0.53        | 0.67       | 0.61       | 0.89       | 2.74       | 1.91       | 0.58        |  |  |           |  |  |  |  |
| Tb                             | 1.6        | 1.9        | 3.3         | 3.2        | 3.1         | 2.5        | 2.1        | 2.2        | 1.8        | 2.5        | 2.1                        | 2.5         | 2.5        | 7.1        | 11.5       | 6.6        | 3.0        | 3.0         |  |  |           |  |  |  |  |
| Yb                             | 0.26       | 0.32       | 0.49        | 0.47       | 0.48        | 0.35       | 0.28       | 0.30       | 0.25       | 0.41       | 0.32                       | 0.34        | 0.34       | 1.18       | 1.55       | 0.90       | 0.44       | 0.44        |  |  |           |  |  |  |  |
| Lu                             | 0.53       | 0.54       | 0.42        | 0.42       | 0.41        | 0.44       | 0.51       | 0.51       | 0.52       | 0.46       | 0.50                       | 0.53        | 0.47       | 0.45       | 0.27       | 0.14       | 0.14       | 0.30        |  |  |           |  |  |  |  |

\* Total iron as FeO

\*\* Analyses by isotope dilution mass spectrometry (see also table 2)

Location key: a - NE of N1, b - quarry between N4 and N5, c - E of N5, d - creek N of Parapebas-Serra Norte Road, e - CVRD drill core, F-87, 174m, f - CVRD drill core, F-32, 173m. See also Figure 2

in the trachyandesites, and might also have been altered.

Mafic rocks show both flat REE and LREE-enriched patterns, normalized to chondrites (Fig. 5). The heavy REE's, exemplified by Yb, correlated well with magnesium number (Fig. 4a), attributed primarily to fractional crystallization. The LREE's show no such correlation (Fig. 4b). Si, K, Rb, Ba, Cs, and LREE are positively correlated through all the mafic rocks, although not linearly (Figs. 3b, 6). Assimilation of a granitic component would add these elements without enriching the Sr, Ti, P, and Ta (contained in more refractory phases), and could thus produce a relative depletion in these latter elements (Fig. 6). Variations in the amounts of such assimilation may account for the many of the differences between basalts and trachyandesites. Some of the latter have magnesium numbers as high as the basalts.

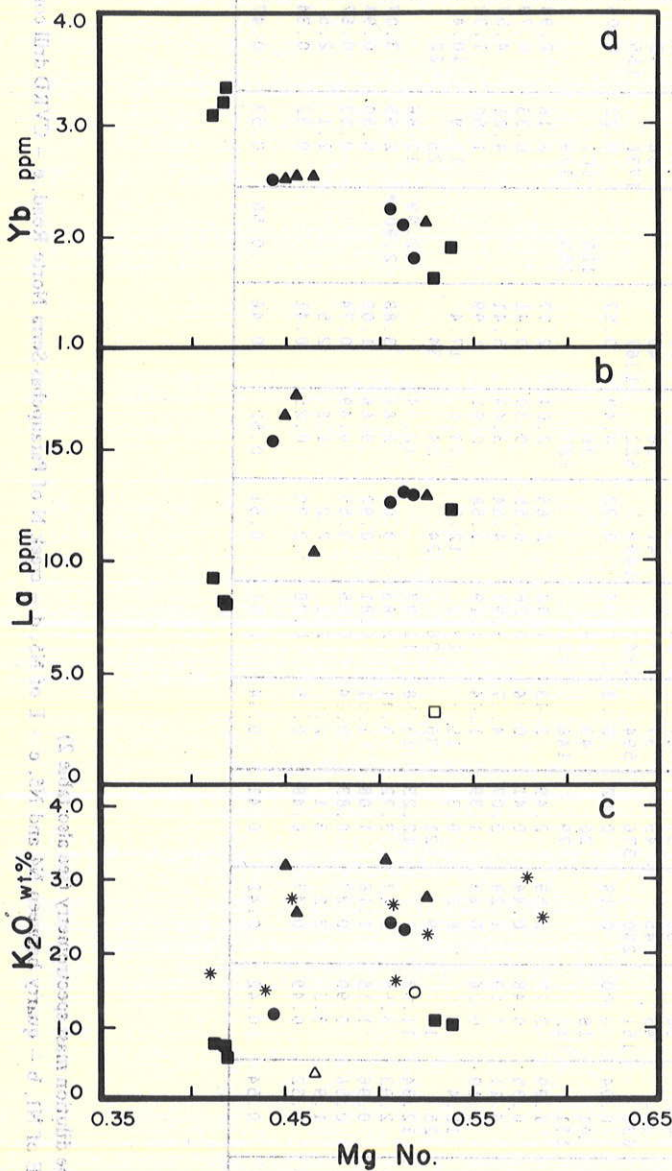


Figure 4 - Variations of elements with magnesium number (atomic ratio Mg : Mg+Fe). Yb and magnesium number are inversely correlated (a), but there is no correlation between La and magnesium number (b). K and magnesium number show a weak positive correlation in both basalts and basaltic andesites (c)

Because of the resistance of many incompatible element ratios to significant modification by magmatic differentiation processes, the relative contents of these elements may help to identify the sources of magma contaminants. Weaver & Tarney (1983), Thompson *et al.* (1983), and Kay (1984) considered several likely types of crustal contaminants and noted that both upper and lower crust have strong enrichment of the larger cations (left side of the figure 6) with distinctive relative depletion of Ta, Sr, P and Ti relative to the other elements. Relative depletion in Th is characteristic of granulite-grade tonalitic gneisses, and in subduction-zone basalts of both island arcs and continental margins. The relative enrichment of the large-radius incompatible elements in the Grão Pará mafic volcanic rocks, without matching enrichments of Th, Ta, Sr, P, and Ti could thus be explained by assimilation of both upper and lower crust. Similar patterns have been shown for many continental flood basalts. It is also

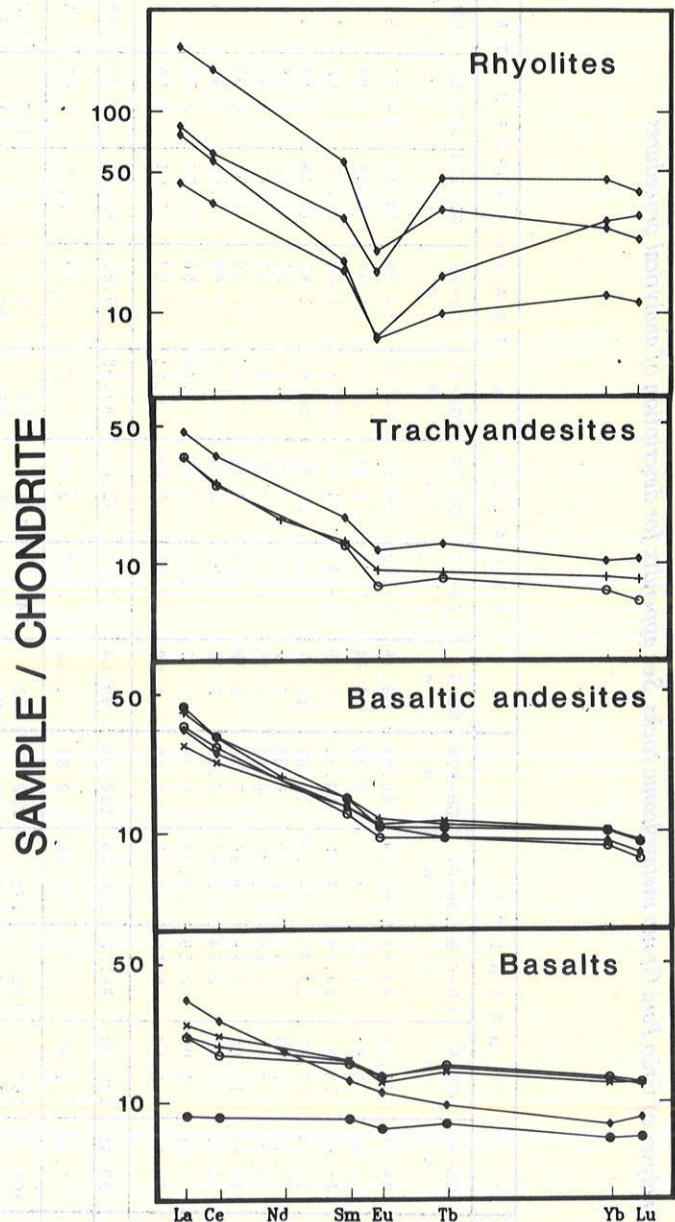


Figure 5 - Rare-earth element diagrams for selected Grão Pará Group basalts, basaltic andesites, trachyandesites, and rhyolites. The two most magnesian basalts have similar low HREE's but very different LREE's

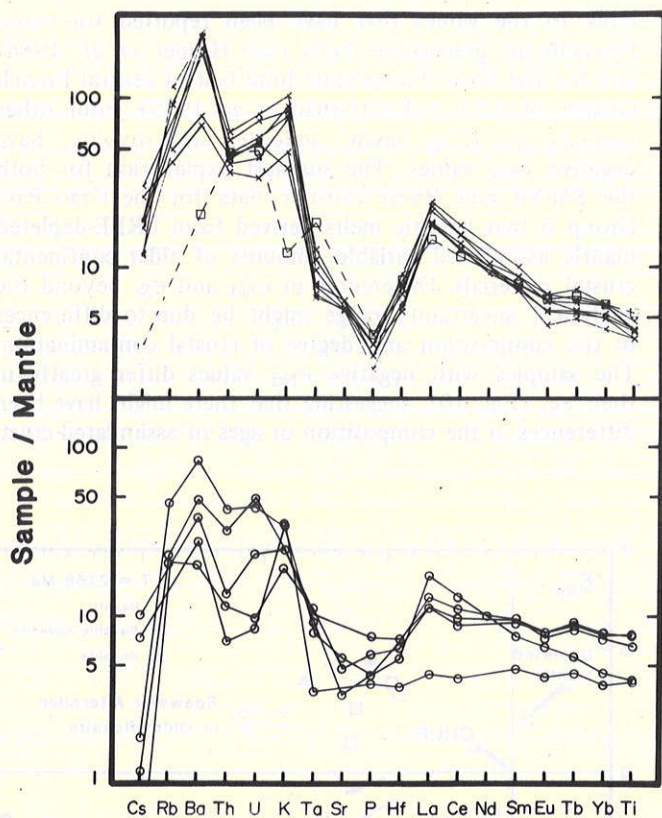


Figure 6 – Incompatible-element diagrams for Grão Pará Group mafic rocks, normalized to the primitive mantle model of Wood et al. (1979), showing the variable enrichments in LREE, K, Rb, Ba, Cs, (and U?), without comparable enrichment in Th, Ta, Sr, P, or Ti. The samples shown with a dashed line contains evidence of spilitization. Karoo basalts show similar enrichment patterns (Norry & Fitton 1983)

possible that these characteristics are inherited from old, trace-element enriched, subcontinental lithosphere, as described by Weaver & Tarney (1983).

**ISOTOPE GEOCHEMISTRY AND AGE** The whole-rock Rb-Sr isotopes in 2 basalts and 5 of the basaltic andesites and trachyandesites plot on an isochron with an age of  $2687 \pm 54$  Ma (MSWD 0.98) (Fig. 7). This age is within the limits of calculated uncertainty of a U-Pb age for zircons from the associated Grão Pará Group rhyolites (see Wirth et al., 1986), suggesting that the Rb-Sr isochron dates the age of volcanism. The initial Sr isotopic ratio of 0.7057 strongly suggests contamination of the mantle-derived melts with continental crust that had evolved with a high Rb/Sr ratio. Although the isochron has a geologically reasonable age, some of the isotopic variation might be influenced by variations in the compositions and amounts of older crustal material assimilated either during magma ascent or hydrothermal cooling. Trans-Amazonian metamorphism might also have affected some of the samples, producing limited scatter from what was originally a single isotopic system. A repeat analysis of sample GB-87, a relatively magnesian basalt with incompatible element enrichment, confirmed that it does not plot on the isochron, indicating the need for caution in interpreting the rest of the Rb-Sr data. If the zircon age of 2758 Ma is used to calculate  $\epsilon_{Sr}$  values for the samples, GB-104 (included in

the isochron) has an unusually low  $\epsilon_{Sr}$  value of +7.0, compared to the average of +45.7 and the very high value of +206.1 in GB-87 is also anomalous. Exclusion of both GB-104 and 87 from the calculation yields an improved isochron with an age of  $2738 \pm 66$  Ma (MSWD 0.69), indistinguishable from the zircon age.

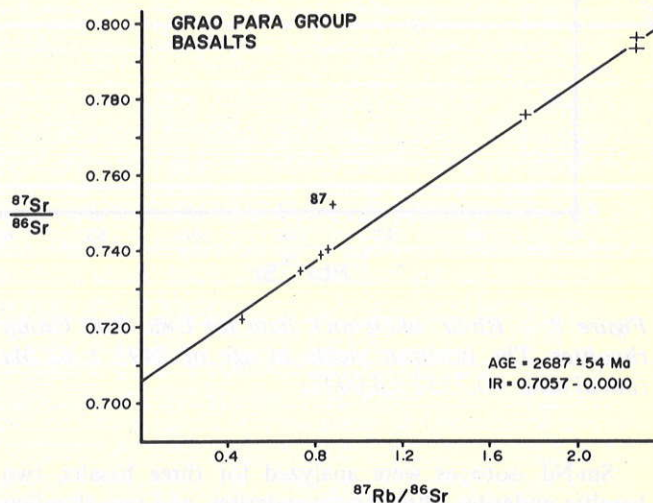


Figure 7 – Rb-Sr whole-rock data for Grão Pará Group mafic rocks. The isochron was computed without sample GB-87

The Rb-Sr data for four rhyolites (Table 2, Fig. 8) show the Sr to be remarkably radiogenic, due to the extremely low Sr contents. The data plot along an isochron of  $2497 \pm 62$  Ma (MSWD 3.68), with an initial ratio of  $0.7152 \pm 0.0052$ . The rhyolite Rb-Sr systems were apparently partially reset long after the volcanism, but they still demonstrate an Archean, pre-Trans-Amazonian age.

Table 2 – Rb, Sr, Sm and Nd concentrations and isotopic ratios of Grão Pará Group basalts, basaltic andesites, trachyandesites and rhyolites. All analyses by Wm. J. Olszewski, Jr., University of New Hampshire, using isotope dilution and mass spectrometry

| Sample  | Rb (ppm) | Sr (ppm) | $\frac{87Rb}{86Sr}$ | $\frac{87Sr}{86Sr}$ | Sm (ppm) | Nd (ppm) | $\frac{147Sm}{144Nd}$ | $\frac{143Nd}{144Nd}$ | $\epsilon_{Sr}$ | $\epsilon_{Nd}$ |
|---------|----------|----------|---------------------|---------------------|----------|----------|-----------------------|-----------------------|-----------------|-----------------|
| GB-67   | 79       | 130      | 1.766               | 0.77515             | 2.70     | 11.97    | 0.13642               | 0.511781              | 48.7            | +3.6            |
| GB-82-a | 20       | 79       | 0.7338              | 0.73456             | 3.55     | 12.23    | 0.17551               | 0.51254               | 57.8            | +4.6            |
| GB-82-b | 18       | 112      | 0.4668              | 0.72214             | 3.55     | 11.82    | 0.18134               | 0.51206               | 32.8            | -7.0            |
| GB-85   | 78       | 99       | 2.282               | 0.79817             | 13.61    | 75.73    | 0.10866               | 0.511286              | 83.1            | +3.8            |
| GB-86   | 36       | 127      | 0.8286              | 0.73871             | 2.76     | 12.34    | 0.13524               | 0.511711              | 63.0            | +2.6            |
| GB-87   | 41       | 131      | 0.9204              | 0.75241             | 2.94     | 12.84    | 0.13869               | 0.511544              | 206.1           | -1.9            |
| GB-93   | 43       | 146      | 0.8604              | 0.74011             | 3.03     | 13.58    | 0.13507               | 0.511634              | 64.9            | +1.2            |
| GB-94   | 48       | 7        | 22.25               | 1.48964             | 3.25     | 15.82    | 0.12437               | 0.511352              |                 | -0.6            |
| GB-95   | 62       | 12       | 16.39               | 1.2998              |          |          |                       |                       |                 |                 |
| GB-102  | 101      | 130      | 2.274               | 0.79519             | 2.70     | 11.86    | 0.13776               | 0.511789              | 45.2            | +3.2            |
| GB-104  | 120      | 155      | 2.270               | 0.79237             | 2.90     | 12.99    | 0.13700               | 0.511483              | 7.2             | -1.8            |
| GB-124  | 97       | 6        | 53.88               | 2.7365              |          |          |                       |                       |                 |                 |

$\epsilon_{Nd}$  and  $\epsilon_{Sr}$  computed using an age of 2758 Ma. Sr CHUR value = 0.701197.

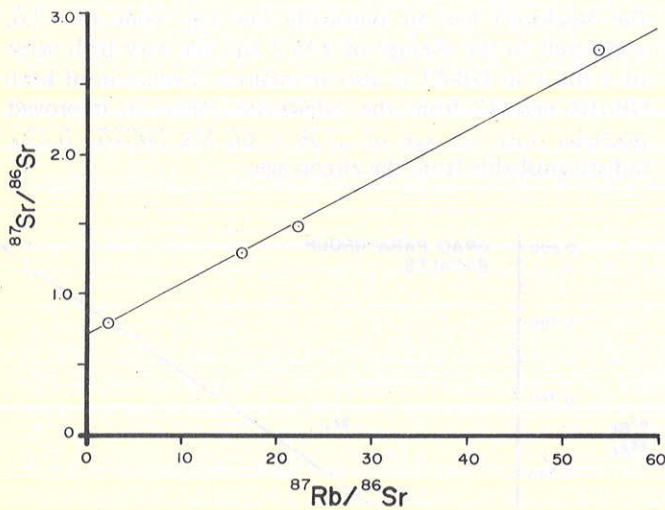


Figure 8 - Rb-Sr whole-rock data for Grão Pará Group rhyolites. The isochron yields an age of  $2497 \pm 62$  Ma (initial ratio =  $0.7152 \pm 0.0052$ )

Sm-Nd isotopes were analyzed for three basalts, two basaltic andesites, three trachyandesites, and two rhyolites (Table 2). The data are too scattered to yield an isochron (Fig. 9). If the zircon age of 2758 Ma is used, their  $\epsilon_{Nd}$  values relative to CHUR range from -7.0 to +4.6, and average about +0.6. Analytical uncertainties in the Sm-Nd system are about 0.8  $\epsilon$  units ( $2\sigma$ ), thus most of the scatter is not analytical. Similar scatter in  $\epsilon_{Nd}$ , with relatively constant Sm/Nd ratios occurs in the Tertiary Skye basalts, and this has been attributed to variable amounts of crustal assimilation (Thirlwall & Jones 1983).

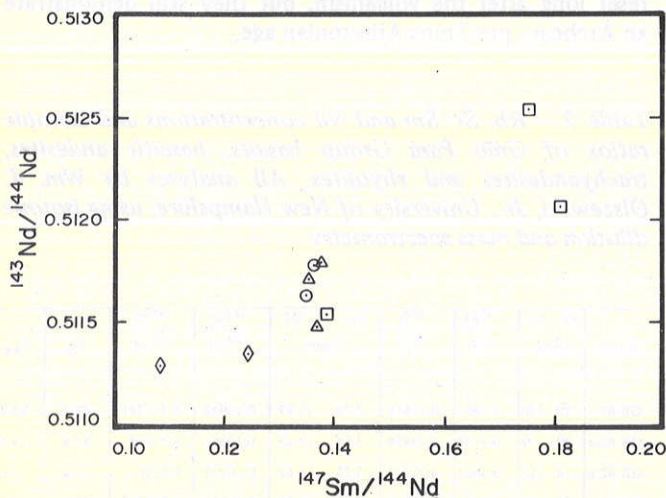


Figure 9 - Sm-Nd isotope data for Grão Pará Group metavolcanic rocks. The symbols are the same as in figure 2. No isochron has been calculated because of the scatter of the samples. The slope of the distribution is compatible with an Archean age of the samples

The  $\epsilon_{Nd}$  values of one basalt, one rhyolite, and four of the andesitic rocks are in the range of +2.6 to +4.6, compa-

rable to the values that have been reported for many Precambrian greenstone belts (see Hegner *et al.* 1984) and for the Early Proterozoic Inini belt of central French Guiana of  $+2.1 \pm 1.8$  (Gruau *et al.* 1985). Four other samples, including basalt, andesite, and rhyolite, have negative  $\epsilon_{Nd}$  values. The simplest explanation for both the Sm-Nd and Rb-Sr isotopic data for the Grão Pará Group is that basaltic melts derived from LREE-depleted mantle assimilated variable amounts of older continental crustal materials. Differences in  $\epsilon_{Nd}$  and  $\epsilon_{Sr}$  beyond the analytical uncertainty range might be due to differences in the composition and degree of crustal contamination. The samples with negative  $\epsilon_{Nd}$  values differ greatly in their  $\epsilon_{Sr}$  (Fig. 10), suggesting that there might have been differences in the composition or ages of assimilated crust.

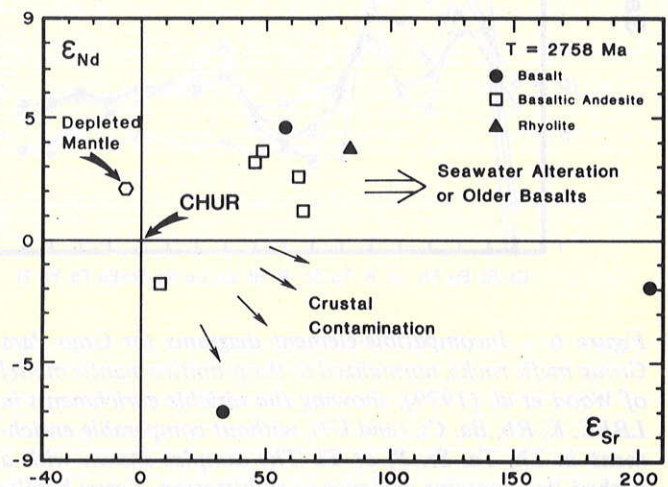


Figure 10 -  $\epsilon_{Sr}$  -  $\epsilon_{Nd}$  diagram for Grão Pará Group metavolcanic rocks

**DISCUSSION** The Grão Pará volcanics yield strong geochemical and isotopic evidence of their incorporation of older continental crust. The bimodal distribution of mafic rocks and rhyolites, and the compositions of the mafic rocks are features in common with both ancient and modern continental volcanic provinces. They differ from the basalts of most Archean greenstone belts, modern oceans and subduction complexes, and alkali basalts of modern hot spots. The Grão Pará Group mafic rocks have the chemical characteristics of continental basalts, like those of the Karoo (Cox 1983, Norry & Fitton 1983), the British Tertiary Province (Dickin *et al.* 1984), the Mesozoic basalts of the eastern United States, the Basin and Range province (e.g. Suneson & Lucchita 1983), and the Parana Basin in Brazil (Belleini *et al.* 1984, Fodor *et al.* 1985a, 1985b, Mantovani *et al.* 1985). The volcanic suite is bimodal, lacking the intermediate compositions that are typically abundant in subduction complexes. In comparison with oceanic basalts, Grão Pará rocks have much higher K, Rb, Ba, and LREE contents. In comparison with alkali basalts, the Grão Pará rocks are relatively deficient in Th, Nb, Sr, P, and Ti abundances. These characteristics are generally attributed to assimilation of older continental



crustal material, either during the ascent of the magmas through the crust or due to subduction of crustal material into mantle source areas.

Other suites of Precambrian continental volcanics share the geochemical characteristics of bimodal silica distribution and LREE and alkali enrichment. The Pongola volcanics, in the oldest continental cover sequence in southern Africa are chemically comparable (Hegner *et al.* 1981). Proterozoic volcanics on the periphery of the Canadian Superior Province also have many of these characteristics (Greenberg & Brown 1983, Francis *et al.* 1983). The Grão Pará mafic rocks have generally higher alkali contents than either of these other Precambrian suites. The Fortescue Group in western Australia, overlying and peripheral to the Pilbara craton and underlying the Hammersley iron deposits, also consists of several kilometers of dominant basalts and felsic volcanics (Hickman 1983).

The Grão Pará volcanics are chemically distinct from two suites of LREE- and alkali-enriched volcanics that have been described from many greenstone belts. Sun & Nesbitt (1978) identified a common type of spinifex-textured Archean basalt with LREE-enriched and flat HREE patterns. These have relative depletion in P and Ti, and often relative enrichment in K, Rb, Ba, but the alkali enrichments are much lower than in the Grão Pará mafic volcanics. The Grão Pará basalts might have started from similar material in the mantle, but they are now clearly distinct from this class of greenstone belt rocks. They are also unlike the relatively rare alkaline volcanic rocks in the upper sequences of several of the Archean greenstone belts of Canada (Ujike 1985, Hubregste 1976), South Africa (Condie & Baragar 1974) and Finland (Jahn *et al.* 1980). These alkaline suites are not restricted to mafic and rhyolitic compositions and they are much more highly alkaline than the Grão Pará Group.

Some of the other important iron-bearing sequences of South America and adjacent west Africa are also Archean, and further comparative studies of these are warranted. The Imataca Complex in Venezuela and the Liberian in west Africa are both Archean, and contain metavolcanic and metasedimentary sections with extensive iron formations (Kalliokoski 1965, Dougan 1977, Ascanio 1981, Cahen *et al.* 1984). Though at higher metamorphic grade, the quartzites and marbles in the Imataca Complex indicate that it was also formed on continental crust, and Montgomery (1977) found that the lead in the Imataca iron formations is unusually radiogenic, possibly reflecting a continental source. The Nova Lima Group in Minas Gerais might be compared with the Grão Pará Group, because it also includes metavolcanic rocks, iron formation, manganese formation, and auriferous chemical metasediments, and is also Archean (Dorr 1973, Thorpe *et al.* 1984). The Nova Lima Group differs in several significant respects from the Grão Pará Group: it has been repeatedly metamorphosed, it is considered a eugeosynclinal assemblage, much of its iron formation is carbonate, and its iron is of subordinate

importance compared to the unconformably overlying Minas Supergroup.

Two other major Precambrian continental basin sequences with significant iron formations also share many of the lithostratigraphic and geochemical characteristics of the Serra dos Carajás belt. Early Proterozoic basins surrounding the Canadian Superior Province have these characteristics. The Fortescue Group in western Australia contains basalts, rhyolites, and underlies the Hammersley iron formations, and clastic, continental sedimentary rocks. The Fortescue Group has been recently dated at  $2.76 \pm 0.03$  Ga (Richards & Blockley 1984, Pidgeon 1984). The discovery that the Grão Pará Group and the Fortescue Group in Australia are both Archean substantially modifies the geological record of deposition of major iron formations. Both were formerly considered Proterozoic. Iron formations were evidently deposited in extensive, ensialic basins in the Late Archean as well as in the Early Proterozoic, which had formerly been considered the major era for deposits of this type.

**APPENDIX: Sample preparation and analytical methods** Rock samples were crushed in a steel jaw crusher, and pulverized in tungsten carbide shatterboxes. Major element compositions were determined by wavelength-dispersive electron microprobe analyses of glasses fused from pulverized rocks. The siliceous volcanics were fluxed with lithium tetraborate. Rare earth elements (except for Nd) and trace elements (except for Rb and Sr) were obtained by instrumental neutron activation, calibrated against standard rock powders. Cobalt and tantalum contamination occurs with the tungsten carbide pulverizing, and the values shown are minima, having been corrected using empirical ratios between tungsten and these trace elements. Rb and Sr values were obtained by isotope dilution, and are estimated to have precisions of about 2% and 0.5% of the reported values, respectively. Isotope dilution Sm and Nd precisions are estimated at about 1% of the reported values.

**Acknowledgments** The field work was made possible by the generous support of Docegeo. We thank Breno Augusto dos Santos and Darcy Lindenmayer for their support and permission, and Edivaldo Miereles for his support and guidance in the field. Our work also benefitted from discussions of the regional geology with other Docegeo geologists, and N. Villas and J.F. Ramos (Universidade Federal do Pará) and J.M. Danni (Universidade Federal Brasília); analytical advice from Sue and Robert Kay (Cornell); and discussion of the isotopic data with Henri Gaudette (New Hampshire). This material is based on work supported by the U.S. National Science Foundation under Grant No. EAR-8410379 to Allan Gibbs. Most of this material is presented and discussed further in Karl Wirth's M.Sc. dissertation. William Olszewski, Jr. is primarily responsible for the Rb-Sr and Sm-Nd analyses and interpretation.

#### REFERENCES

- AMARAL, G. - 1974 - *Geologia Pré-Cambriana da Região Amazônica*. São Paulo, (Tese de Livre Docência, Inst. Geoc. USP), 212 p.
- AMARAL, G. - 1984 - Províncias Tapajós e Rio Branco. In: ALMEIDA, F.F.M. de & HASUI, Y. ed. *Pré-Cambriano do Brasil*, São Paulo, Blücher, p. 6-35.
- ASCANIO, G. - 1981 - Yacimientos de mineral de hierro del Precambriaco de Venezuela. In: SYMPOSIUM AMAZÔNICO, Puerto Ayacucho, 1981, *Atas...* Puerto Ayacucho, Venezuela, March 22-30, (preprint) 22 p.

- BEISIEGEL, V.R.; BERNADELLI, A.L.; DRUMMOND, N.F.; RUF, A.W.; TREMAINE, J.W. - 1973 - Geologia e Recursos Minerais da Serra dos Carajás. *Rev. Bras. Geoc.*, 3(4):215-242.
- BEISIEGEL, V.R. - 1982 - Distrito ferrífero da Serra dos Carajás. In: BERNARDELLI, A.L. (Coord.), *Província Mineral de Carajás - Pará*. In: SIMP. GEOL. AMAZÔNIA, 1, Belém, 1982. *Anais...*, Belém, SBG/N.Norte, p. 21-46 (Anexo).
- BELLEINI, G.; BROTZU, P.; COMIN-CHIARAMONTI, P.; ERNETSO, M.; MELFI, A.; PACCA, I.G.; PICCIRILLO, E.M. - 1984 - Flood basalt to rhyolite suites in the Southern Paraná plateau (Brazil): Paleomagnetism, petrogenesis and geodynamic implications. *J. Petrology*, 25:579-618.
- BERNARDELLI, A.L. - 1982 - Jazida de manganês do Azul. In: BERNARDELLI, A.L. (Coord.), *Província Mineral de Carajás - Pará*. In: SIMP. GEOL. AMAZÔNIA, 1, Belém, 1982. *Anais...*, Belém, SBG/N.Norte, p. 47-59 (Anexo).
- CAHEN, L.; SNELLING, N.J.; DELHAL, J.; VAIL, J.R. - 1984 - *The Geochronology and Evolution of Africa*. Oxford, Clarendon Press, 512 p.
- CONDIE, K.C. & BARAGAR, W.R.A. - 1974 - Rare-earth element distributions in volcanic rocks from Archean greenstone belts. *Contrib. Mineral. Petrol.*, 45:237-246.
- CORDANI, U.G.; TASSINARI, C.C.G.; KAWASHITA, K. - 1984 - A Serra dos Carajás como região llimitrofe entre províncias tectônicas. *Ciências da Terra*, (9):6-11.
- COX, K.G. - 1983 - The Karoo province in southern Africa: Origin of trace element enrichment patterns. In: HAWKESWORTH, C.L. & NORRY, M.J. ed. *Continental Basalts and Mantle Xenoliths*. Cheshire, U.K., Shiva Publ. Ltd., p. 5-19.
- DICKIN, A.P.; BROWN, J.L.; TROMPSON, R.N.; HALLIDAY, A.N.; MORRISON, A.A. - 1984 - Crustal contamination and the granite problem in the British Tertiary Volcanic Province. *Phil. Trans. R. Soc. Lond.*, 310-A:755-780.
- DORR, J.V.N. II - 1973 - Iron-formation in South America. *Econ. Geol.* 68:1005-1022.
- DOUGAN, T. - 1977 - The Imataca Complex near Cerro Bolivar, Venezuela - calc-alkaline Archean Protolith. *Precamb. Res.*, 4:237-268.
- FARIAS, N.F. & SEUERESSIG, R. - 1982 - Pesquisa geológica da jazida de cobre Salobro 3A. In: SIMP. GEOL. AMAZÔNIA, 1, Belém, 1982. *Anais...*, Belém, SBG/N.Norte, p. 39-45.
- FERREIRA FILHO, C.F. & DANNI, J.C.M. - 1985 - Petrologia e mineralizações sulfetadas de Prospecto Bahia - Carajás. In: SIMP. GEOL. AMAZÔNIA, 2, Belém, 1985. *Anais...*, Belém, SBG/N.Norte, v. 3, p. 34-47.
- FIGUEIRAS, A.J.M. & VILLAS, R.N.N. - 1982 - Estudo petrológico e sedimentológico da Sequência Clástica (Pós-Grupo Grão Pará) da Serra dos Carajás, Estado do Pará. In: CONGR. BRAS. GEOL., 32, Salvador, 1982. *Anais...*, Salvador, SBG, v. 2, p. 832-846.
- FODOR, R.V.; CORWIN, C.; ROISENBERG, A. - 1985a - Petrology of Serra Geral (Paraná) continental flood basalts, southern Brazil: crustal contamination, source material, and South Atlantic magmatism. *Contrib. Mineral. Petrol.*, 91:54-65.
- FODOR, R.V.; CORWIN, C.; SIAL, A.N. - 1985b - Crustal signatures in the Serra Gral flood-basalt province, southern Brazil: O- and Sr-isotope evidence. *Geology*, 13:763-765.
- FRANCIS, D.; LUDDEN, J.; HYNES, A. - 1983 - Magma evolution in a Proterozoic rifting environment. *J. Petrology*, 24:556-582.
- GIBBS, A.K.; WIRTH, K.; HIRATA, W.K. - 1985 - *Field report on a visit to the Grão Pará Group, Serra dos Carajás, Brazil*. Belém, Docegeo, 35 p. (Unpublished report).
- GOMES, C.B.; CORDANI, U.G.; BASEI, M.A.S. - 1975 - Radiometric Ages from the Serra dos Carajás Area, Northern Brazil. *Geol. Soc. Amer. Bull.*, 86:939-945.
- GREENBERG, J.K. & BROWN, B.A. - 1983 - Lower Proterozoic volcanic rocks and their setting in the southern Lake Superior district. *Geol. Soc. Amer. Memoir*, 160:67-84.
- GRUAU, G.; MARTIN, H.; LEVEQUE, B.; CAPDEVILA, R. - 1985 - Rb-Sr and Sm-Nd geochronology of Lower Proterozoic granite-greenstone terrains in French Guiana, South America. *Precamb. Res.*, 30:63-80.
- HEGNER, E.; TEGTMEYER, A.; KRONER, A. - 1981 - Geochemie und petrogenese archaischer Vulkanite der Pongola-Gruppe in Natal, Sudafrika. *Chem. Erde*, 40:23-57.
- HEGNER, E.; KRONER, A.; HOFFMAN, A.W. - 1984 - Age and isotope geochemistry of the Archean Pongola and Usushawna suites in Swaziland, southern Africa: a case for crustal contamination of mantle-derived magma. *Earth Planet. Sci. Lett.*, 70:267-279.
- HICKMAN, A.H. - 1983 - Geology of the Pilbara Block and its environs. *Geol. Surv. West. Austral. Bull.*, 127, 268 p.
- HIRATA, W.K.; RIGON, J.C.; KADEKARU, K.; CORDEIRO, A.A.C.; MEIRELES, E.A. - 1982 - Geologia regional da província mineral de Carajás. In: SIMP. GEOL. AMAZÔNIA, 1, Belém, 1982. *Anais...*, Belém, SBG/N.Norte, p. 100-110.
- HUBREGSTE, J.J.M.W. - 1976 - Chemistry of cyclic subalkaline and younger shoshonitic volcanism in the Knee Lake - Oxford Lake greenstone belt, northeastern Manitoba. Manitoba Dept. Mines, Min. Res. Div., *Geol. Paper*, 78(2), 18 p.
- JAHN, B.M.; AUVRAY, B.; BLAIS, S.; CAPDEVILA, R.; CORNICHE, J.; VIDAL, F.; HAMERURT, J. - 1980 - Trace element geochemistry and petrogenesis of Finnish greenstone belts. *J. Petrology*, 21:201-244.
- KALLIOKOSKI, J.O. - 1965 - Geology of north-central Guyana Shield, Venezuela. *Geol. Soc. Amer. Bull.*, 76:1027-1050.
- KAY, R.W. - 1984 - Elemental abundances relevant to identification of magma sources. *Phil. Trans. R. Soc. Lond.*, 310-A:535-548.
- LEMOS, V.P. & VILLAS, R.N. - 1983 - Alteração das rochas básicas de Grupo Grão Pará-implicações sobre a gênese de depósito de bauxita de N5, Serra dos Carajás. *Rev. Bras. Geoc.*, 13(3):165-177.
- MANTOVANI, S.M.; MARQUES, L.S.; DE SOUSA, M.A.; CIVETTA, L.; ATALLA, L.; INNOCENTI, F. - 1985 - Trace element and strontium isotope constraints on the origin and evolution of Paraná continental flood basalts of Santa Catarina State (Southern Brazil). *J. Petrology*, 26:187-209.
- MEDEIROS NETO, F.A. & VILLAS, R.N.N. - 1985 - Geologia da jazida de Cu-Zn do corpo 4E-Pojuca, Serra dos Carajás. In: SIMP. GEOL. AMAZÔNIA, 2, Belém, 1985. *Anais...*, Belém, SBG/N. Norte, v. 3, p. 97-112.
- MONTGOMERY, C.W. - 1977 - *Uranium-lead isotopic investigation of the Archean Imataca Complex, Guayana Shield, Venezuela*. Cambridge, Massachusetts, (Unpub. Ph.D. Diss., Massachusetts Institute of Technology), 261 p.
- NORRY, M.J. & FITTON, J.G. - 1983 - Compositional differences between oceanic and continental basic lavas and their significance. In: C.L. HAWKESWORTH & M.J. NORRY. ed. *Continental Basalts and Mantle Xenoliths*. Cheshire, U.K., Shiva Publ. Ltd., p. 5-19.
- PIDGEON, R.T. - 1984 - Geochronological constraints on early volcanic evolution of the Pilbara Block, Western Australia. *Austral. J. Earth Sci.*, 31:237-242.
- RAMOS, J.F.F.; MOURA, C.A.V.; MELO, C.F.; PEREIRA, J.L.; SERIQUE, J.S.C.B.; RODRIGUES, R.M. - 1984 - Uma discussão sobre seqüências sedimentares tidas como formação Rio Fresco, Sudeste do Pará. (preprint).
- RICHARDS, J.R. & BLOCKLEY, J.G. - 1984 - The base of the Fortescue Group, Western Australia: Further galena lead isotope evidence on its age. *Aust. J. Earth Sci.*, 31:257-268.
- SANTOS, J.O.S. & LOGUERCIO, S.O.C. - 1984 - A parte Meridional do Craton Amazônico (Escudo Brasil-Central e as Bacias do Alto Tapajós e Parecis-Alto Xingu. In: SCHOBBERNHAUS, C. et al., ed. *Geologia do Brasil*. Brasília, DNPM, p. 93-127.
- SANTOS, B.A. dos - 1981 - *Amazônia: Potencial Mineral e Perspectivas de Desenvolvimento*. São Paulo, EDUSP, 256 p.
- SILVA, G.G.; LIMA, M.I.C.; ANDRADE, A.R.F.; ISSLER, R.S.; GUIMARÃES, G. - 1974 - *Folha SB.22-Araguaia e parte de folha SC.22-Tocantins*. Projeto Radam, DNPM, Rio de Janeiro, *Levantamento de Recursos Naturais*, v. 4, p. 13-143.
- SUN, S.S. & NESBITT, R.W. - 1978 - Petrogenesis of Archean ultrabasic and basic volcanics: Evidence from rare-earth elements. *Contrib. Mineral. Petrol.*, 65:301-325.
- SUNESON, N.H. & LUCCHITA, I. - 1983 - Origin of bimodal volcanism, southern Basin and Range province, west-central Arizona. *Geol. Soc. Amer. Bull.*, 91:1005-1019.
- TASSINARI, C.C.G.; HIRATA, W.K.; KAWASHITA, K. - 1982 - Geologic evolution of the Serra dos Carajás, Pará, Brazil. *Rev. Bras. Geoc.*, 12:263-267.
- THIRLWALL, M.F. & JONES, N.W. - 1983 - Isotope geochemistry and contamination mechanics of Tertiary lavas from skye, northwest Scotland. In: HAWKESWORTH, C.L. & NORRY, M.J. ed. *Continental Basalts and Mantle Xenoliths*. Cheshire,

U.K., Shiva Publ. Ltd., p. 186-208.  
 THOMPSON, R.N.; MORRISON, M.A.; DICKIN, A.P.; HENDRY, G.L. - 1983 - Continental flood basalts... Arachnids rule OK? In: HAWKESWORTH, C.L. & NORRY, M.J. ed. *Continental Basalts and Mantle Xenoliths*. Cheshire, U.K., Shiva Publ. Ltd., p. 158-185.  
 THORPE, R.I.; CUMMING, G.L.; KRSTIC, D. - 1984 - Lead isotope evidence regarding age of gold deposits in the Nova Lima district, Minas Gerais, Brazil. *Rev. Bras. Geoc.*, 14(3): 147-152.  
 TOLBERT, G.E.; TREMAINE, J.W.; MELCHER, G.C.; GOMES, C.B. - 1971 - The recently discovered Serra dos Carajás iron deposits, northern Brazil. *Econ. Geol.*, 66:985-994.  
 UJIKE, O. - 1985 - Geochemistry of Archean alkalic volcanic rocks from the Crystal Lake area, east of Kirkland Lake, Ontario, Canada. *Earth Planet. Sci. Lett.*, 73:333-344.  
 WEAVER, B.L. & TARNEY, J. - 1983 - Chemistry of the subcon-

tinental mantle: inferences from archean and proterozoic dikes and continental flood basalts. In: HAWKESWORTH, C.L. & NORRY, M.J. ed. *Continental Basalts and Mantle Xenoliths*. Cheshire, U.K., Shiva Publ. Ltd., p. 209-229.  
 WIRTH, K.R.; GIBBS, A.K.; OLSZEWSKI JR., W.J. - 1986 - U-Pb zircon ages of the Grão Pará Group and Serra dos Carajás Granite, Pará, Brazil. *Rev. Bras. Geoc.*, 16(2):195-200.  
 WOOD, D.A.; JORON, J.L.; TREUIL, M.; NORRY, M.; TARNEY, J. - 1979 - Elemental and Sr isotope variations in basic lavas from Iceland and the surrounding ocean floor. *Contrib. Mineral. Petrol.*, 70:319-339.

MANUSCRITO

Recebido em 10 de janeiro de 1986

Revisão aceita em 09 de setembro de 1986

Há uma coisa mais importante do que as mais belas descobertas: é o conhecimento do método pelo qual são feitas.

Leibniz, apud Asmus 1983 (Série Projeto REMAC 6)